The random-coil 'C' fragment of the dihydropyridine receptor II–III loop can activate or inhibit native skeletal ryanodine receptors

Claudia S. HAARMANN[1], Daniel GREEN, Marco G. CASAROTTO, Derek R. LAVER[2] and Angela F. DULHUNTY[3]

Muscle Research Group, John Curtin School of Medical Research, Australian National University, P.O. Box 334, Canberra, ACT 2601, Australia

The actions of peptide *C*, corresponding to ^{724}Glu–Pro^{760} of the II–III loop of the skeletal dihydropyridine receptor, on ryanodine receptor (RyR) channels incorporated into lipid bilayers with the native sarcoplasmic reticulum membrane show that the peptide is a high-affinity activator of native skeletal RyRs at cytoplasmic concentrations of 100 nM–10 μM. In addition, we found that peptide *C* inhibits RyRs in a voltage-independent manner when added for longer times or at higher concentrations (up to 150 μM). Peptide *C* had a random-coil structure indicating that it briefly assumes a variety of structures, some of which might activate and others which might inhibit RyRs. The results suggest that RyR activation and inhibition by peptide *C* arise from independent stochastic processes. A rate constant of 7.5×10^5 s$^{-1} \cdot$ M^{-1} was obtained for activation and a lower estimate for the rate constant for inhibition of 5.9×10^3 s$^{-1} \cdot$ M^{-1}. The combined actions of peptide *C* and peptide *A* (II–III loop sequence ^{671}Thr–Leu^{690}) showed that peptide *C* prevented activation but not blockage of RyRs by peptide *A*. We suggest that the effects of peptide *C* indicate functional interactions between a part of the dihydropyridine receptor and the RyR. These interactions could reflect either dynamic changes that occur during excitation–contraction coupling or interactions between the proteins at rest.

Key words: DHPR–RyR interaction, dihydropyridine receptor (DHPR) II–III loop, excitation–contraction coupling, peptide *C*, ryanodine receptor (RyR).

INTRODUCTION

Excitation–contraction (EC) coupling is the translation of an action potential on the surface membrane of a muscle fibre into Ca^{2+} release from the internal sarcoplasmic reticulum (SR) Ca^{2+} store, to trigger muscle contraction. Two Ca^{2+} channels are important in this signal transmission: the dihydropyridine receptor (DHPR) and the ryanodine receptor (RyR). The DHPR spans the transverse tubular membrane, detects action potential depolarization and communicates the depolarization to the RyR Ca^{2+}-release channel in the SR membrane.

The mechanism of signalling between the two proteins differs between cardiac and skeletal muscle. In cardiac muscle, a depolarization-induced Ca^{2+} current through the DHPR initiates Ca^{2+}-induced Ca^{2+} release from the SR [1–3]. In contrast, in skeletal muscle the surface Ca^{2+} current is not necessary for EC coupling [4]. Instead, there is an interaction between the DHPR and RyR, requiring the cytoplasmic loop region between transmembrane repeats II and III of the skeletal DHPR α_1 subunit (^{666}Glu–Leu^{791}) [5]. Residues ^{725}Phe–Pro^{742} of the skeletal II–III loop are essential for skeletal-type EC coupling in myocytes [6–8].

In isolated systems the skeletal II–III loop can activate [^{3}H]ryanodine binding to SR vesicles and single RyR channels [9]. Peptides corresponding to two regions of the II–III loop can activate RyRs. Peptide *A* (^{671}Thr–Leu^{690}) increases Ca^{2+} release from, and [^{3}H]ryanodine binding to, the SR as well as single RyR activity [10–13]. The increased RyR activity in SR vesicles is associated with an increase in methylcoumarin acetate fluorescence [14], indicating that peptide *A* binding causes a conformational change in the RyR protein. Peptide *A* has a strong helical structure [15]: it activates single RyR channels at > 1 μM, but blocks the channel pore at higher concentrations [10,13]. Peptide *C*, corresponding to ^{724}Glu–Pro^{760}, activates Ca^{2+} release from SR [16] and activates purified skeletal RyR channels [13] and, although it does not inhibit Ca^{2+} release from SR vesicles, peptide *C* inhibits the activation of Ca^{2+} release by peptide *A* [17]. In this study, we have examined the actions of peptide *C* on native RyR channels incorporated into lipid bilayers with their co-protein (12 kDa forkhead-505-binding protein) and associated proteins (e.g. junctin, triadin, calsequestrin and other anchored proteins) attached [18–20]. The effects of peptides on native RyR channels, which more closely mimic the RyR channel complex *in vivo*, have not previously been described. Preliminary data have been presented [21].

The aim of the present experiments was to define the interactions between the *C* region of the II–III loop and the native RyR channel and to resolve the apparent conflict between the excitatory effects of peptide *C* on RyR channels and the inhibitory effect that prevents activation of Ca^{2+} release by peptide *A* in SR vesicle studies. We explored the possibility that peptide *C* (an acidic peptide) prevents activation of RyRs by the basic peptide *A* by binding to, and hence masking basic residues on peptide *A* which are essential for its binding to the RyR [15]. This is the first examination of (i) the functional interactions between peptide *C* and single native RyR channels in lipid bilayers, (ii) simultaneous regulation of single native RyRs by peptides *A* and *C* and (iii) the structure of peptide *C*. Novel findings are (i) peptide *C* can both activate and inhibit native RyR channels via two independent

Abbreviations used: RyR, ryanodine receptor; DHPR, dihydropyridine receptor; EC, excitation–contraction; SR, sarcoplasmic reticulum; PE, phosphatidylethanolamine; PS, phosphatidylserine; PC, phosphatidylcholine; DIDS, di-isothiocyanostilbene-2′,2′-disulphonic acid.

[1] Present address: Department of Anatomy and Neurobiology, Colorado State University, Fort Collins, CO 80523-0001, U.S.A.

[2] Present address: School of Biomedical Science, Faculty of Health, University of Newcastle, Newcastle, NSW 2308, Australia.

[3] To whom correspondence should be addressed (e-mail angela.dulhunty@anu.edu.au).

stochastic processes, (ii) peptide *C* prevents the activation, but not the blockage, of RyRs in lipid bilayers by peptide *A* and (iii) peptide *C* has a random-coil structure in solution. In addition, we show for the first time that the peptide *C* does not bind directly to peptide *A*. Finally, the ability of peptide *C* to inhibit native RyR channels (this study) but not purified RyR channels [13] raises the novel concept that co-proteins or associated proteins may play a role in functional interactions between the *C* region of the II–III loop and the RyR.

MATERIALS AND METHODS

Isolation of SR vesicles

Back and leg muscles were removed from New Zealand White rabbits, and SR vesicles were prepared as described previously [18,22]. Heavy SR vesicles were collected from the 35–45 % (w/v) interface of a discontinuous sucrose gradient, centrifuged, resuspended and stored in liquid N_2 or at -70 °C.

Peptides

Peptides, synthesized as described previously [10], had the following sequences. Peptide *A*: ^{671}Thr-Ser-Ala-Gln-Lys-Ala-Lys-Ala-Glu-Glu-Arg-Lys-Arg-Arg-Lys-Met-Ser-Arg-Gly-Leu^{690}. Peptide *C*: ^{724}Glu-Phe-Glu-Ser-Asn-Val-Asn-Glu-Val-Lys-Asp-Pro-Tyr-Pro-Ser-Ala-Asp-Phe-Pro-Gly-Asp-Asp-Glu-Glu-Asp-Glu-Pro-Glu-Ile-Pro-Val-Ser-Pro-Arg-Pro-Arg-Pro^{760}.

Lipid bilayers and solutions

Bilayers were formed and vesicles incorporated as described previously [22,23]. Bilayers were composed of phosphatidylethanolamine (PE), phosphatidylserine (PS) and phosphatidylcholine (PC) in a ratio of PE/PS/PC = 5 : 3 : 2 unless otherwise stated. SR vesicles (10 μg/ml) added to the *cis*-chamber using *cis* and *trans* solutions containing 20 mM CsCl, 0.1 mM $CaCl_2$ and 10 mM Tes (pH 7.4 adjusted with CsOH) as well as either *cis*/*trans* 230 mM/230 mM caesium methanesulphonate, plus 500 mM/0 mM mannitol or 230 mM/30 mM caesium methanesulphonate. Channel activity was recorded with symmetrical 250 mM/250 mM Cs^+. Potentials are expressed as $V_{\text{cytoplasm}}$–V_{lumen} (i.e. V_{cis}–V_{trans}).

Recording and analysis of single-channel data

Recording and analysis have been described previously [22,23]. Channel activity was recorded at +40 and −40 mV for ⩾ 30 s under control conditions and for several minutes after peptide addition. Estimates of channel activity were based on the mean current (I') through the channels, calculated using the software package Channel2 (written by P. W. Gage and M. Smith, Australian National University, Canberra, ACT, Australia). The magnitude of channel activity is measured by the fractional mean current (I'_F):

$$I'_F = I'/I'_{max} \quad (1)$$

where I'_{max} is the maximum open conductance. Changes in channel activity are given by the relative mean current (I'_{rel}):

$$I'_{rel} = I'_F(\text{test})/I'_F(\text{control}). \quad (2)$$

Solution exchange

Solutions were exchanged by perfusion using back-to-back syringes. The efficiency of exchange was determined spectrophotometrically at 710 nm, by dilution of 1 mM Antipirylazo III (in distilled water) during perfusion with different volumes of distilled water. Perfusion with 11 ml of solution (≈ 6 vol.) gave ≈ 1000-fold dilution and perfusion with 6 ml (≈ 4 vol.) gave 10–20-fold dilutions.

Bilayers containing multiple RyR channels

In some experiments, bilayers containing 5–64 RyR channels were used to examine average effects of peptide *C* on RyR activity. Multiple incorporations were achieved using vesicles that had been subjected to several cycles of freezing and thawing. In these experiments the *cis*-solutions contained 230 mM caesium methanesulphonate, 20 mM CsCl, 10 mM Tes and 0–1 mM Ca^{2+}. *Trans*-solutions contained 30 mM caesium methanesulphonate, 20 mM CsCl, 10 mM Tes and 0–100 μM Ca^{2+}. In the inhibition experiments channels were initially maximally activated by exposure to 500 μM di-isothiocyanostilbene-2′,2′-disulphonic acid (DIDS) [24]. Solution exchange in these experiments was by local perfusion techniques [25], modified for rapid solution-exchange times of < 2 s [26].

NMR and CD spectroscopy

Peptide *C* was dissolved in 10 % ^2H_2O/90 % water to a final concentration of ≈ 2 mM at pH 5.0 and NMR spectroscopy performed as described previously [15]. For CD, peptides were diluted to 25 μM in water with a final pH of 4.8. Ten spectra per sample were collected at 5 °C on a Jobin Yvon CD6 Dichrograph using a cell pathlength of 0.2 mm, averaged and subjected to a smoothing function.

Ultracentrifugation

Sedimentation equilibrium experiments were performed in a Beckman Optima XL-A analytical ultracentrifuge using 12-mm-pathlength cells with carbon-filled double sector centre pieces. The solution sector contained 100 μl of sample at ≈ 1 mg/ml in bilayer solution, the solvent sector 110 μl of the same solution as a reference. All experiments were at 20 °C and 282 240 rev./min. Scans were collected and superimposed at 2 h intervals. The absorbance data was analysed using software supplied with the instrument, XLAEQ.

Statistics

Average data are presented as means ± S.E.M. The significance of differences was determined with Student's *t* test ($P \leqslant 0.05$) or the 'sign' test [27].

RESULTS

Peptide *C* can activate and inhibit single RyR channels

The channel in Figure 1 was activated by cytoplasmic peptide *C* at 10 μM. The increase in activity was maintained at 10 and 30 μM peptide and for ≈ 50 s with 50 μM peptide before inhibition became apparent. The mean current (I') with 10, 30 and 50 μM peptide (measured within the first 50 s of exposure to 50 μM *C*) was significantly greater than activity in the control, or with 0.1 or 1.0 μM peptide; the least significant difference was $P < 8 \times 10^{-3}$ from populations of consecutive I' (averages over 5 s segments) tested against each other ($n \geqslant 8$). I' after 50 s with 50 μM peptide fell significantly ($P < 2 \times 10^{-5}$) and was significantly less ($P < 7 \times 10^{-3}$) than I' under control conditions or with 1.0 μM peptide. Similar activation, followed by inhibition, was seen in 6 of 8 channels where the peptide concentration

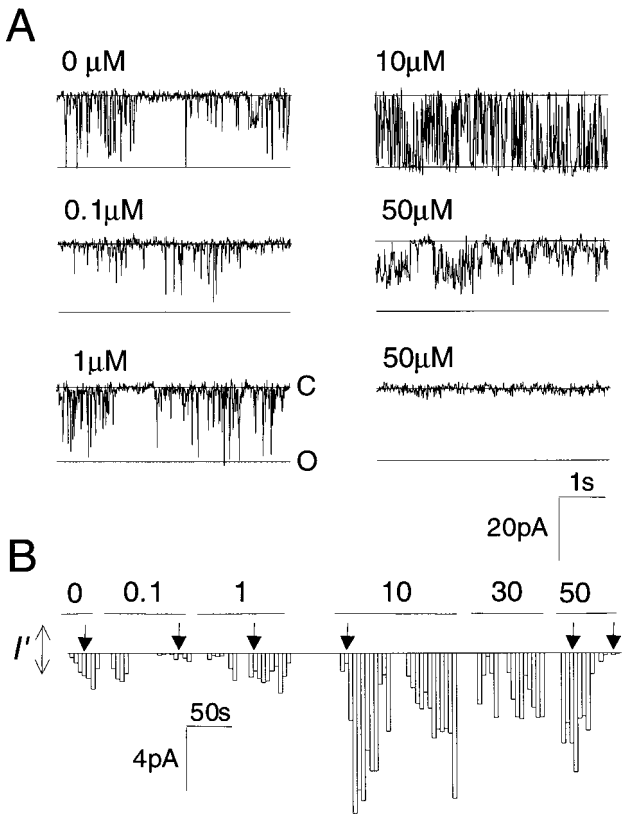

Figure 1 Peptide *C* activates and then inhibits most single RyR channels in lipid bilayers in a concentration-dependent manner

The composition of the bilayer in this and subsequent figures was PE/PS/PC = 5 : 3 : 2 unless otherwise stated (see the Materials and methods section). Exposure of RyRs to low concentrations (1–10 μM) of peptide led to activation. Application of high concentrations (50 μM) led to inhibition. (**A**) Current traces recorded at − 40 mV in the presence of 0.1, 1, 10 and 50 μM peptide *C*. The first record at 50 μM was obtained 15 s after the addition of peptide C and the second record at 50 μM was obtained after 55 s. (**B**) History plot showing mean currents I' in the presence of the indicated peptide *C* concentrations (in μM) at − 40 mV (recording times at + 40 mV are included in the time axis but data are not plotted). Each bin shows I' of a 5 s record. Arrows in (**B**) indicate the intervals that are shown in (**A**). Activity is shown at − 40 mV in symmetric 250 mM Cs^+ and 0.1 mM Ca^{2+}. In (**A**), upper solid lines (labelled C) indicate the closed level of the channel and lower solid lines (labelled O) indicate the maximum unitary conductance.

was increased stepwise from low concentrations. The relative mean current (I'_{rel}) increased with activation between 1.2- and 10-fold in individual channels at concentrations between 0.1 and 50 μM peptide *C*, with an average increase of ≈3-fold (Table 1). Evaluation of activity of channels exposed to a single peptide *C* concentration showed that channel activity with 100 nM peptide was significantly greater than the control ($I'_{rel} = 1.4 \pm 0.2$; $n = 6$; see Figure 3B, below), even though activation with 100 nM peptide was not seen in the particular channel shown in Figure 1. Activation of ≈3-fold was similar in individual channels exposed to 1, 10, 30 and 50 μM peptide *C*. Inhibition either reduced channel activity to submaximal conductances or eliminated activity (Figures 2A–2C). A total of 19 out of 23 channels were inhibited at 50–150 μM peptide *C* within 2 min (Figure 2D). Inhibition was also seen in a few experiments (eight out of 22) when channels were exposed to lower peptide *C* concentrations of 1–30 μM (Figure 2E). There was no correlation between the effects of peptide *C* and the SR vesicle preparation, the level of control channel activity or the experimental conditions. In all cases, $|R^2|$ was $\leqslant 0.4$ for activation and $\leqslant 0.3$ for inhibition.

Table 1 Activation of channels ($n = 8$) by peptide *C* (0.1–50 μM) at + 40 and − 40 mV

Comparison of average data for mean currents (I'), maximum unitary currents (I'_{max}) and relative mean current (I'_{rel}). The difference in the change in I' (under control conditions and in the presence of peptide *C*) and I'_{rel} is due to the different averaging processes: I'_{rel} is the average of the individual relative currents whereas I' is the average over individual experiments under the different conditions.

		I' (pA)	I'_{max} (pA)	I'_{rel}
+ 40 mV	Control	0.6 ± 0.3*	17.6 ± 0.3	–
	Peptide *C*	1.2 ± 0.5*	18.1 ± 0.5	4.8 ± 2.0†
− 40 mV	Control	− 1.7 ± 0.5*	− 19.1 ± 0.8	–
	Peptide *C*	− 4.0 ± 0.9*	− 19.4 ± 0.4	4.6 ± 1.4†

* Indicates significant differences for data obtained at + 40 and − 40 mV.
† Indicates significant differences of $I'_{F(peptideC)}$ from $I'_{F(control)}$.

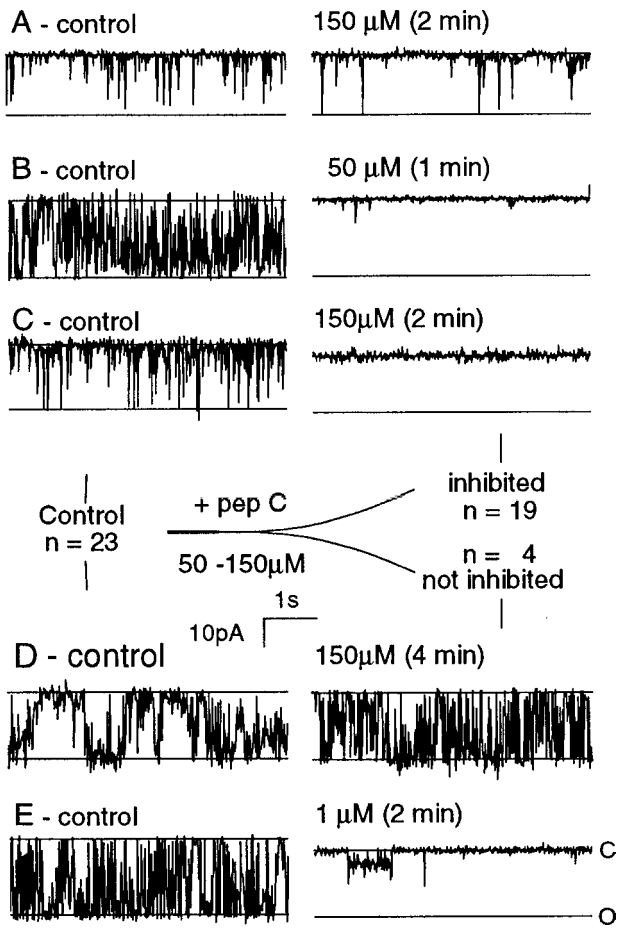

Figure 2 Effect of high peptide *C* concentrations on RyR activity

A total of 19 out of 23 channels were inhibited by peptide *C* between 50 and 150 μM. Inhibition reduced the number of openings (**A**), increased the fraction of openings to submaximal conductance levels (**B**) or abolished activity (**C**). (**D**) Shows a channel that was not inhibited by 150 μM peptide *C* within 4 min. (**E**) Shows a channel that was inhibited by 1 μM peptide *C*. Times above the traces on the right indicate the period of peptide *C* application at the indicated concentration. Activity is shown at − 40 mV in symmetric 250 mM Cs^+ and 0.1 mM Ca^{2+}. Upper solid lines (labelled C) indicate the closed level of the channel and lower solid lines (labelled O) indicate the maximum unitary conductance.

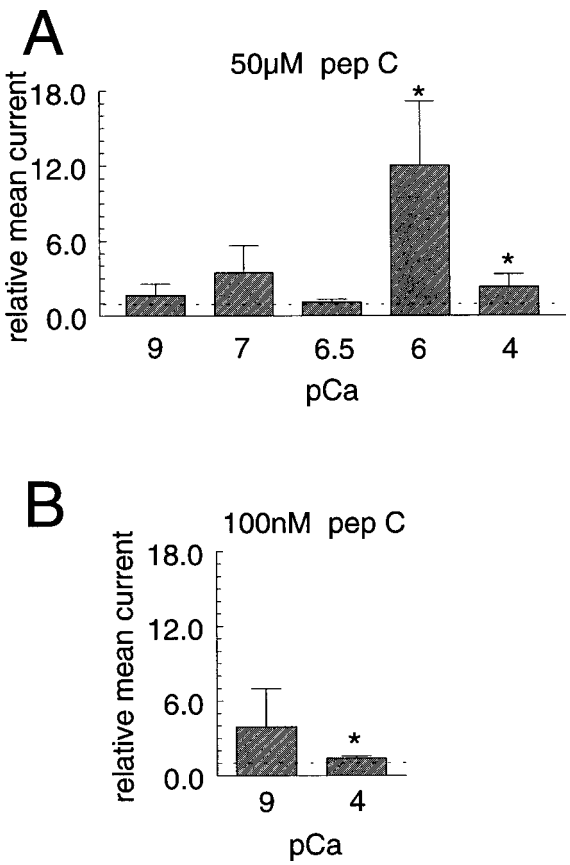

Figure 3 Activation of RyR channels by peptide *C* at different *cis* Ca^{2+} concentrations

(**A**) Effects of 50 μM peptide *C* at various Ca^{2+} concentrations. Data are shown as relative mean current (I'_{rel}). I'_{rel} data with 100 μM *cis* Ca^{2+} was obtained from single-channel experiments similar to those shown in Figure 1. The data with 1 nM–1 μM (*p*Ca 9–6) *cis* Ca^{2+} were obtained from multi-channel experiments, such as those shown in Figure 5 below, to obtain measurable activity under control conditions. (**B**) Effects of 100 nM peptide *C* at *p*Ca 4 and *p*Ca 9. Data were obtained from multi-channel experiments. For multi-channel experiments, the average mean current for individual channels was determined by dividing the mean bilayer current (determined by threshold analysis; see the Materials and methods section) by the number of channels present in the bilayer. The number of channels in the bilayer was determined at the end of the experiment from the maximum current in the presence of ATP and Ca^{2+}. The average data from the experiments was weighted by the number of channels in the bilayer. In (**A**), the numbers of experiments were: *p*Ca 9, $n = 8$; *p*Ca 7, $n = 4$; *p*Ca 6.5, $n = 12$; *p*Ca 6, $n = 9$; *p*Ca 4, $n = 4$. In (**B**), $n = 4$ for *p*Ca 4 and $n = 6$ for *p*Ca 9.

The ability of peptide *C* to release Ca^{2+} from SR vesicles was observed only with very low (10–30 nM) cytoplasmic Ca^{2+} concentrations [16]. Thus we repeated the experiments in bilayers containing multiple RyR channels (with local perfusion techniques: see also below) over a range of *cis* Ca^{2+} concentrations (Figure 3). In contrast to the release of Ca^{2+} from SR vesicles, the effect of 50 μM peptide was significant only at activating *cis* Ca^{2+} concentrations of 1 μM (*p*Ca 6) and 100 μM (*p*Ca 4), although a small increase in channel activity was seen in seven out of eight channels at *p*Ca 9 (Figure 3A). When a very low concentration of peptide was used (100 nM, compared with 10–100 μM required to alter Ca^{2+} release [16]), the mean current tended to increase more at *p*Ca 9 ($n = 4$ channels) than at *p*Ca 4 ($n = 6$ channels), although the increase was not significant. Note that, whereas there was a small relative increase in activity in many channels at *p*Ca 9, the open probability of the channels was very low both before and after peptide addition ($I'_F \approx 0.001$–0.005), and was well

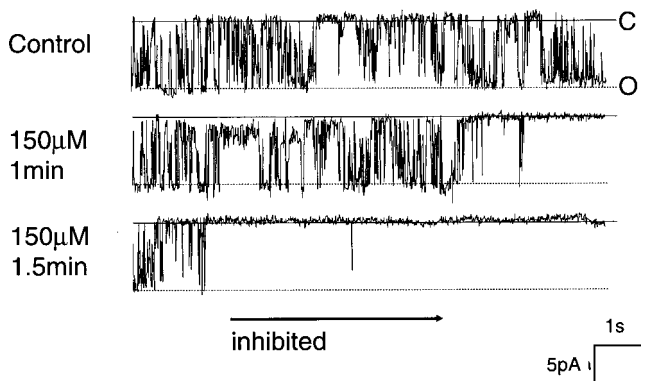

Figure 4 RyR channels could be inhibited by peptide *C*, without prior activation

An example of one of the single channels that was inhibited after a 1.5 min exposure to 150 μM peptide *C*, without any initial activation, is shown. The times given for the second and third traces are the times after addition of peptide *C*. Activity is shown at -40 mV in symmetric 250 mM Cs^+ and 0.1 mM Ca^{2+}. Solid lines indicate the closed level of the channel (labelled C) and broken lines the unitary conductance (labelled O). Similar results were obtained in six experiments (see text).

below levels of activation expected either during EC coupling or from increased Ca^{2+} release from SR or [^{3}H]ryanodine binding.

In these experiments, inhibition was not observed because of the relatively short exposure times to the peptide in all cases and because of the low peptide concentration when 100 nM peptide was used.

Activation and inhibition by peptide *C* occur independently

Although some channels were activated and then inhibited by peptide *C*, there was no correlation between the degree of activation and inhibition in the channels exhibiting both effects. In several instances one or other of activation or inhibition was absent. In six experiments, RyR exposure to one concentration of peptide *C* for several minutes did not increase channel activity prior to inhibition (all six channels showed control and inhibited activity similar to that shown in Figure 4). In three other experiments, RyRs that were initially activated by high concentrations of peptide *C* did not show subsequent inhibition (Figure 5A). One channel was exposed to 30 μM peptide *C* for 2.5 min, one exposed to 50 μM peptide *C* for 2.5 min and the third exposed to 50 μM peptide *C* for 6 min. Together these data strongly suggest that activation and inhibition occur through independent mechanisms.

Time course of activation and inhibition

The time course of peptide *C* effects following aliquot addition to the *cis*-chamber did not accurately reflect the time course of peptide *C* binding to the RyR because of the slow rates of mixing (20 s stirring) and diffusion to the bilayer surface. Therefore rates of activation and inhibition were measured using local perfusion techniques in which the solution in contact with the bilayer could be exchanged fully in < 2 s [26]. An average 2-fold increase in relative mean current was observed in 17 experiments when 100 nM peptide *C* was added under conditions where activity was initially low [with 100 μM Ca^{2+} on either side of the bilayer (Figures 6A and 6C)]. A single exponential fit to the data gave a time constant for activation, τ_a, of 13.3 ± 0.9 s.

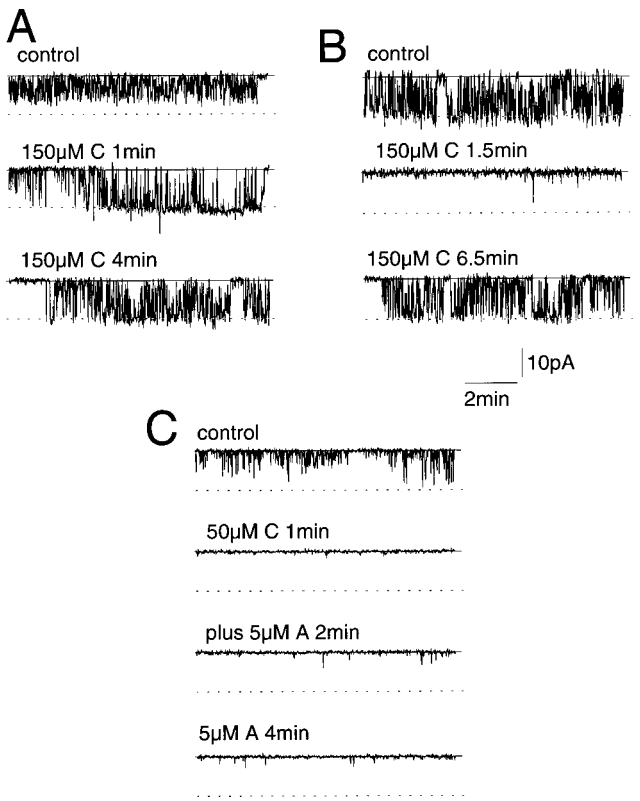

Figure 5 Peptide *C* can (A) cause activation without inhibition, (B) unbind from its inhibition site and (C) prevent activation by peptide *A*

Channel activity is shown at −40 mV. In (**A**) a channel is activated by after 1 min exposure to 150 μM peptide *C* (second trace) and remained activated for 4 min (third trace). In (**B**) a channel is inhibited after a 1.5 min exposure to 150 μM peptide *C* (second trace), activity remained low for 3 min and then recovered to control levels indicating that peptide *C* dissociated from its binding site. In (**C**), a channel was inhibited 1 min after exposure to 50 μM peptide *C* (second trace). Some subconductance activity returned 2 min after subsequent exposure to 5 μM peptide *A* (third trace) and could be observed for a further 2 min (fourth trace). In each example, the bilayer broke shortly after the last trace shown, so that subsequent effects of the peptides were not observed.

Inhibition with 50 μM peptide *C* was observed in 14 experiments in which channel activity was initially high [500 μM DIDS was added to increase activity to a P_O value (the probability of channel opening) close to 1.0] [24] (Figures 6B and 6D), or in channels activated by Ca^{2+} (100 μM free Ca^{2+}) and ATP (2 mM) in one experiment (in contrast to the activation induced by 50 μM peptide *C* when RyR activity was initially low, in the absence of DIDS treatment, described above). The average time constant for inhibition, τ_i, was 3.4 ± 0.2 s. This is likely to be an overestimate of the time constant given that exchange time for the solution was 2 s (above). These results, and the observations that activation and inhibition can proceed independently, suggest that two independent stochastic processes can account for the effects of peptide *C* on RyR channel activity with apparent rate constants for activation of $7.5 \times 10^5\ s^{-1} \cdot M^{-1}$ and for inhibition of $> 5.8 \times 10^3\ s^{-1} \cdot M^{-1}$. This model is consistent with the fact that inhibition was only rarely seen at low peptide concentrations, because the half inhibition time would be slower than the lifetime of the experiments ($\approx$ 3 min with 1 μM peptide or 30 min for 100 nM peptide, and presumably slower in bath perfusion experiments). The fraction of inhibited RyRs increased as peptide *C* concentration increased (Figure 6E). This indicates either that the channel is inhibited when the peptide is bound to both activation and inhibition sites, or that once peptide is bound in its inhibitory conformation it cannot be displaced by peptide in an activating conformation.

Activation and inhibition of RyRs remain after washout of peptide *C*

Neither activation nor inhibition was easily reversed upon washout of peptide *C*. In six experiments 10 μM peptide *C* was removed before the onset of inhibition. Channel activity in five cases remained high (at activated levels shown in Figure 1 and in average activation data in Table 1) for 3–6 min before the bilayer broke, and activity declined in one channel after 1 min. This slow reversal indicates strong association of the peptide with the activation site, with a time constant for dissociation of at least 300 s. Washout of peptide *C* after inhibition did not restore activity after 3.5 min in six out of seven experiments (activity remained at the inhibited levels, e.g. Figures 2A–2C, right-hand panels). 'Control-like' activity (e.g. Figures 2A–2C, left-hand panels) returned in one channel. These observations suggested that the peptide also did not readily dissociate from its inhibition site.

By analogy with other inhibiting drugs with slow kinetics, channel activity in the presence of the inhibitor should show periods of activity when the drug dissociates from its binding site. In eight out of 22 experiments, RyRs showed periods of normal activity (Figure 5B) during exposure to peptide *C*, which occurred between 2.5 and 30 min after inhibition on-set, but in 14 channels activity did not return to control levels between 1 and 28 min (activity continued at the inhibited levels shown in Figure 2). The infrequent periods of activity during inhibition again indicates that the dissociation rate was very slow.

Peptide *C* structure

The structure of peptide *C* was examined using NMR and CD. The amide–amide regions in the NMR two-dimensional NOESY spectra of peptide *C*, in either aqueous media or trifluoroethanol/water mixture (to promote secondary structure; Figure 7B), failed to show the off-diagonal signals reflecting secondary structure. The simplicity of cross peaks in the amide-α region also indicates a lack of one predominant structure (Figure 7A). Maxima and minima in the CD spectra, which indicate a helical structure for peptide *A*, were not seen for peptide *C* (Figure 7C). Thus peptide *C* has a random-coil structure and therefore adopts different conformations, each maintained briefly. The peptide may only occasionally achieve the structure necessary to bind to activation or inhibition sites or to activate or inhibit at one site. This means that the concentration of peptide *C* in its active conformation is in fact lower than that indicated by the total concentration of the peptide.

Peptide *C* does not aggregate in solution

Peptide aggregation at high concentrations might generate peptide *C* complexes that produce RyR inhibition. However, equilibrium sedimentation showed that the peptide did not aggregate at 120–720 μM. The absorbency data yielded a molecular mass of 4400 ± 600 Da, comparable with the monomeric mass of 4183 Da.

Voltage independence of the actions of peptide *C*

Although the low-affinity inhibition by peptide *C* was initially reminiscent of the effects of peptide *A* [10], the effects of peptide

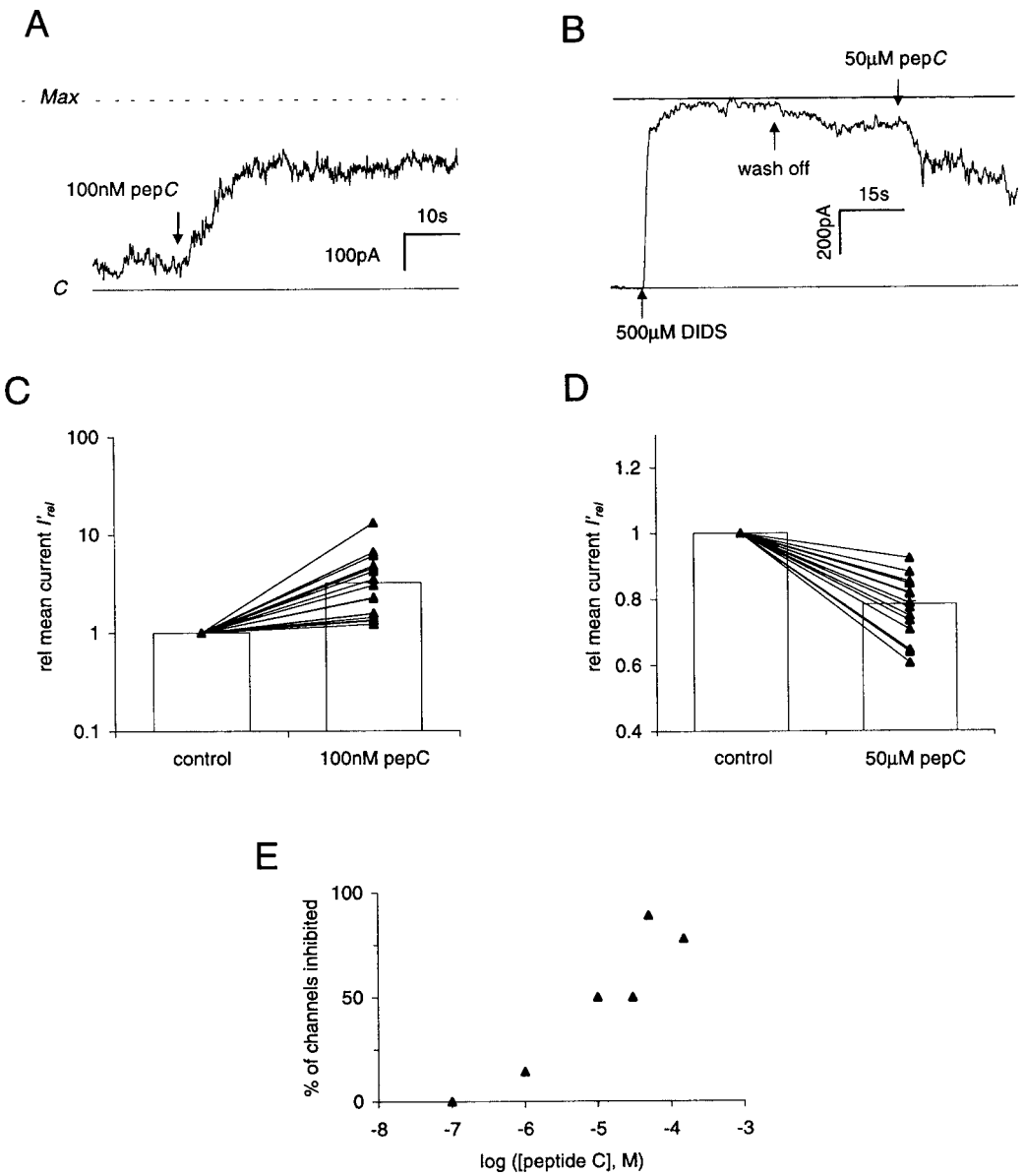

Figure 6 Activation and inhibition of RyR by peptide *C* observed in multi-channel recordings

(**A**) Shows a current trace recorded from a bilayer (PE/PC = 7 : 2) containing ≈ 50 channels at + 40 mV with *cis*/*trans* values of 250 mM/50 mM Cs^+ and 0.1 mM/0.1 mM Ca^{2+}. Channels were exposed to 100 nM peptide *C* at the indicated time. Similar results were obtained in 12 experiments, summarized in (**C**). (**B**) Shows a current trace recorded from a bilayer having the usual composition of PE/PS/PC = 5 : 3 : 2 containing ≈ 40 channels at + 40 mV with *cis*/*trans* values of 250 mM/50 mM Cs^+ and 0.1 mM/0 mM Ca^{2+}. Channels were activated by 500 μM DIDS, which was then washed off. Channels were exposed to 50 μM peptide *C* at the indicated time. Similar results were obtained in 13 experiments, summarized in (**D**). In (**A**) C and the solid line denote the baseline, Max and the broken line indicate the maximum current observed during the experiments. (**C**) and (**D**) show the relative mean current (I'_{rel}) of individual experiments (symbols connected by lines), and weighted means ± S.E.M. (histograms). * indicates that data are significantly different from data under control conditions. (**E**) The fraction of RyRs inhibited (within 180 s of exposure) increases with peptide *C* concentration (determined from single-channel records).

C were not voltage-dependent, whereas the block by peptide *A* depends on the voltage and direction of current flow. Indeed, both activation and inhibition were similar at + 40 and − 40 mV (Tables 1 and 2).

This voltage independence indicates that inhibition is not due to a block of the pore and is consistent with peptide *C* having a net negative charge and thus not being attracted to the negatively charged residues in the RyR pore. The results imply that inhibition of RyRs by peptides *C* and *A* occurs at different sites.

Inhibition by peptide *C* prevents activation of RyRs by ATP and peptide *A*

We investigated the possibility that RyR activators, such as ATP and peptide *A*, could activate channels that were inhibited by peptide *C*. Exposure of peptide *C*-inhibited channels to ATP (2 mM) for up to 2.5 min did not increase RyR ($n = 3$; activity remained at inhibited levels illustrated in Figure 2). Peptide *A* (5 μM) appeared to increase the frequency of openings to subconductance openings at − 40 mV, in three of five cases

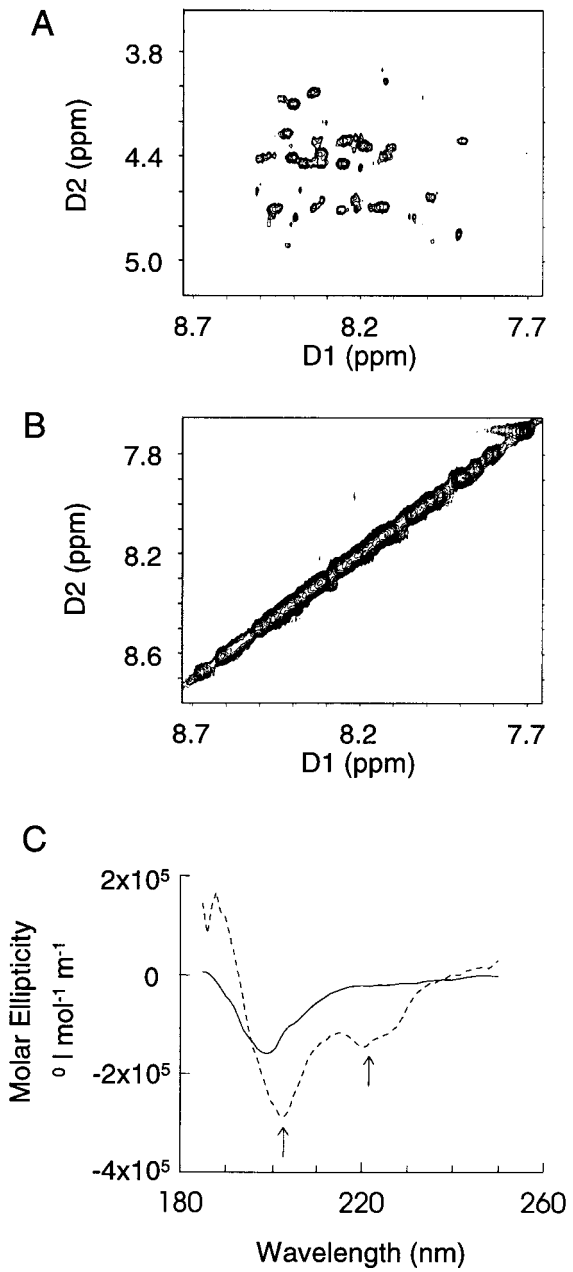

Figure 7 Structural studies of peptide *C*

NMR spectra suggest that peptide *C* has a random-coil structure. (**A**) Amide-α and (**B**) amide–amide regions of the NOESY ^{1}H spectrum (mixing time, 200 ms) of peptide *C* in 10 % ^2H_2O/90 % water at 25 °C, pH 5.0. Cross peaks in the amide–amide spectra and the simplicity of the amide-α spectra indicate the lack of secondary structure. CD spectra suggest that peptide *C* does not form a helical structure. Absorbance (molar ellipticity) is plotted against the wavelength (nm) for peptide *C* (solid line) and peptide *A* (broken line). Minima at 201 and 222 nm (arrows), indicating helical structure, are seen with peptide *A* [15], but not with peptide *C*. Both peptides *C* and *A* were dissolved in aqueous solution.

(Figure 5C). However, the activity with peptide *C* plus peptide *A* did not increase to the greater than control levels normally seen with peptide *A* in the absence of peptide *C*. Thus inhibition by peptide *C* suppressed activation by ATP (or prevented ATP binding to the RyR) and prevented peptide *A* from activating the RyR to levels greater than that during the initial control activity.

Table 2 Inhibition of channels by peptide *C* at +40 and −40 mV

Comparison of average data of mean current (I'), maximum unitary current (I'_{max}) and relative mean current (I'_{rel}). The difference in the change in I' (under control conditions and in the presence of peptide *C*) and I'_{rel} is explained in Table 1.

		I'(pA)	I'_{max} (pA)	I'_{rel}*
+40 mV	Control	1.61 ± 0.48†	17.8 ± 0.3	
	50 μM peptide *C* (n = 13)	0.25 ± 0.11†	17.6 ± 0.2	0.58 ± 0.29‡
	150 μM peptide *C* (n = 9)	0.10 ± 0.03†	17.8 ± 0.4	0.21 ± 0.10‡
−40 mV	Control	−3.28 ± 0.67†	−18.8 ± 0.4	
	50 μM peptide *C* (n = 13)	−1.33 ± 0.61†	−18.2 ± 1.1	0.77 ± 0.44‡
	150 μM peptide *C* (n = 9)	−0.37 ± 0.25†	−19.2 ± 0.7	0.29 ± 0.19‡

* Errors in this column for +40 mV are S.E.M. estimated from the scatter of I'_{rel} values. The *t* test was not performed on these populations.

† Indicates significant differences of data for +40 and −40 mV.

‡ Indicates significant differences of $I'_{F(peptide C)}$ from $I'_{F(control)}$.

We investigated the effects of peptide *A* and ATP on the activity of RyRs that remained inhibited after peptide *C* had been washed out of the bath, to determine whether peptide *A* could displace peptide *C* from its binding site. This experiment was possible since peptide *C* dissociates very slowly from the RyR (see above), and no recovery from inhibition was seen prior to the addition of either agonist. The effects of ATP and peptide *A* on these inhibited channels were similar to the effects seen on RyRs inhibited in the presence of peptide *C* in the bath. ATP applied for 5 min had no effect in three of five experiments, induced subconductance openings in one channel and restored 'control-like' activity in the other. In addition, peptide *A* induced subconductance openings in three of four experiments ($\leqslant$ 2 min) at −40 mV and restored 'control-like' activity after 40 s in one experiment (but did not increase activity above control). These results suggest that peptide *A* accessed its activation site when peptide *C* was bound to the RyR, but did not displace peptide *C* from its inhibitory site or alter the properties of this binding site.

Activation by peptides *A* and *C* are not additive

The additive effects of peptide *C* and peptide *A* at −40 mV were examined, since peptide *C* prevents peptide *A*-induced Ca^{2+} release from SR [17]. A 5-fold excess of peptide *C* added after peptide *A* did not reduce the peptide *A*-induced activation at −40 mV (Figure 8A). However, when peptide *C* was added before peptide *A* (Figures 8B and 9B), average activity at −40 mV did not increase when peptide *A* was added.

The results in Figures 8(B) and 8(C) do not necessarily suggest specific interactions between peptides *A* and *C*, but rather suggest that superimposing events prevent an average activation by peptide *A* in the presence of peptide *C*. The average ineffectiveness of the initial addition of peptide *C* could be due to simultaneous activation in some channels and inhibition in other channels, as seen in the individual channel data (Figure 8C). Similarly, the lack of activation by peptide *A* can be attributed to summation of time-dependent inhibition by peptide *C* with activation by peptide *A*.

Peptide association in solution

Association between the positively charged peptide *A* and the negatively charged peptide *C* could have prevented activation of RyRs by peptide *A* (above), and its activation of Ca^{2+} release

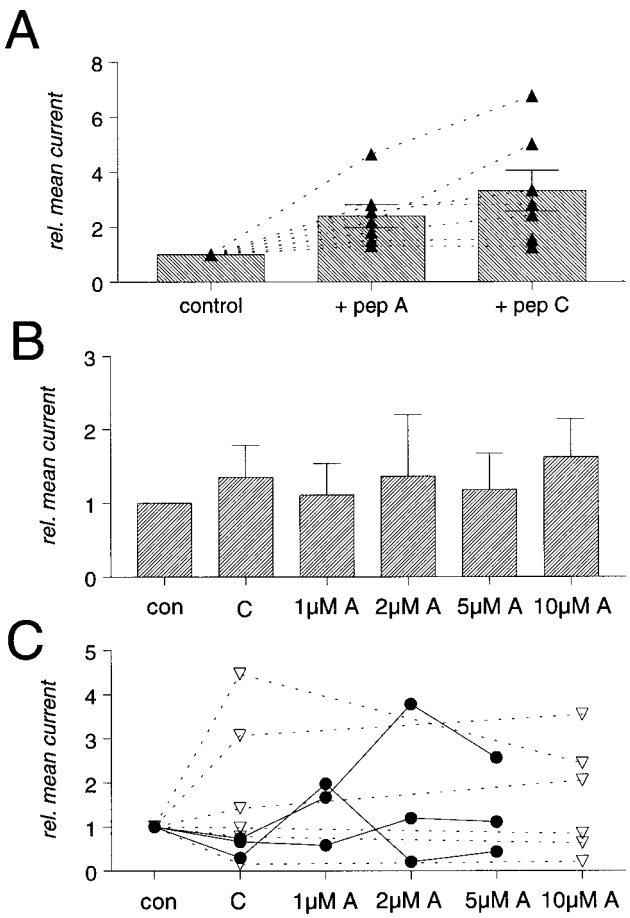

Figure 8 Peptide *C* does not reverse or reduce the activation of RyRs by peptide *A* at −40 mV (if added after peptide *A*), but prevents average activation by peptide *A* (if added before peptide *A*)

In (**A**), I'_{rel} at −40 mV is plotted for control conditions ($I'_{rel} = 1$), after application of activating concentrations of peptide *A* (1–10 μM), and then after application of peptide *C* (at concentrations in at least 5-fold excess over peptide *A*). Peptide *A* significantly activated the RyRs and activity remained high, or tended to increase further after application of peptide *C*. The bins show the average values for the seven experiments, which are also shown individually as data points connected by broken lines. The experiments in (**B**) show average I'_{rel} for nine experiments and in (**C**) show the data from the nine individual channels. The open symbols are for six experiments in which channels were exposed to peptide *C* and then to 10 μM peptide *A*. The filled symbols show three experiments in which channels were exposed to peptide *C* and then to the indicated concentrations of peptide *A* (1, 3 and 5 μM). In (**B**) and (**C**), peptide *C* (30–50 μM) was added for 3 min before peptide *A* (each concentration maintained for 3 min). Peptide *A* did not cause an average increase in RyR activity when added after peptide *C*. Channels were recorded in symmetric 250 mM Cs^+ and 0.1 mM Ca^{2+}.

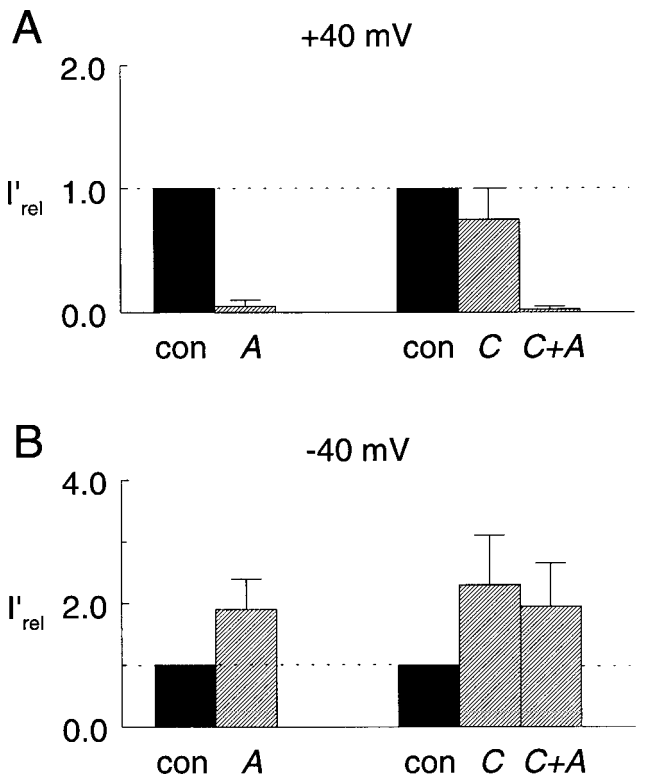

Figure 9 Peptide *C* does not alter blockage of the RyR caused by 10 μM peptide *A* at +40 mV

The average relative mean current (I'_{rel}) is plotted for five experiments in which channels that were exposed to 10 μM peptide *A* and for five experiments in which channels were exposed to 30 or 50 μM peptide *C* before peptide *A* application at +40 mV (**A**) and −40 mV (**B**). The bars show control data for each experiment (con), for peptide *A* alone (*A*), peptide *C* alone (*C*) and peptide *C*+peptide *A* (*C* + *A*). No significant difference between the blockage of RyRs by peptide *A* at +40 mV in the presence and absence of peptide *C* was observed (**A**). Channel activity at −40 mV is increased with peptide *A* in the absence of peptide *C*, but did not increase when peptide *A* was added in the presence of peptide *C*. Channels were recorded in symmetric 250 mM Cs^+ and 0.1 mM Ca^{2+}.

from SR [17]. However, some chemical shifts of peaks in one-dimensional NMR spectra of peptide *A*, corresponding to positively charged residues in peptide *A* that might interact with the negatively charged residues in peptide *C*, did not change during titration with peptide *C* (to equimolarity; Figure 10). Overall, there were no significant spectral changes in peptide *A* (i.e. in chemical shifts or line broadening) spectra shown in Figure 10 that would suggest an interaction between peptides *A* and *C*. In addition sedimentation equilibrium failed to show an increase in molecular mass. The absorbance versus radius data were fitted to a model system of up to three size species of different proportions in the mixture. This showed that the mixture behaved as a non-reacting mixture of components of molecular masses 2000 Da (peptide *A*) and 4000 Da (peptide *C*). There was no evidence of the presence of a component of 6000 Da or higher. Therefore interaction between the effects of the peptides cannot be explained by their association.

The fact that channel blockage by peptide *A* at +40 mV was not reduced by peptide *C* (Figure 9A) also indicated that peptides *A* and *C* did not associate. If peptide *A* associated with peptide *C*, it might have been less effective in blocking the pore because its net charge would have been reduced and its bulk increased. However, this was not the case because channels were inhibited at +40 mV when 10 μM peptide *A* was added $\approx$3.5 min after 30–50 μM peptide *C* (Figure 9A and Table 3). Peptide *C* had not inhibited the channels at the time of addition of peptide *A*. The inhibition by peptide *A* could not be attributed to the continuing presence of peptide *C*, because it was observed only at +40 mV (Figure 9A) and occurred immediately after addition of peptide *A*. There was no change in activity at −40 mV (Figure 9B).

Summary of peptide *C* and peptide *A* effects

The changes in RyR activity with peptides *A* and *C*, either alone or together, are summarized here. (i) Two independent mechanisms produce peptide *C* activation of RyRs and voltage-independent inhibition at low and high concentrations, respectively (Figures 1–4 and 6; Tables 1 and 2). (ii) Another two independent mechanisms

Table 3 Comparison of average data for mean current (I'), maximum unitary current (I'_{max}), relative mean current (I'_{rel}) in five experiments under control conditions, after addition of peptide *C* (30 or 50 μM) followed by addition of peptide *A* (10 μM; columns 3–5) and in another five experiments for control conditions and after addition of peptide *A* alone, i.e. in the absence of peptide *C* (columns 6–8) at + 40 and − 40 mV

Some of the data at − 40 mV are presented in Figure 9(B).

1	2	3 I' (pA)	4 I'_{max} (pA)	5 I'_{rel}*	6 I' (pA)	7 I'_{max} (pA)	8 I'_{rel}*
+ 40 mV	Control	0.68 ± 0.19†	17.0 ± 1.0		2.8 ± 0.9†	17.1 ± 0.6	
	+ peptide *C*	0.46 ± 0.13†	16.8 ± 0.6	0.76 ± 0.25	–	–	
	+ peptide *A*	0.02 ± 0.01	12.4 ± 1.4	0.04 ± 0.01‡	0.09 ± 0.03†	17.1 ± 0.6	0.06 ± 0.03‡
− 40 mV	Control	− 3.6 ± 1.30	− 18.7 ± 0.7		− 2.8 ± 0.8†	− 18.1 ± 0.4†	
	+ peptide *C*	− 5.5 ± 1.3	− 19.1 ± 1.0	2.25 ± 0.80	–	–	
	+ peptide *A*	− 4.3 ± 0.5	− 17.9 ± 0.9	1.88 ± 0.58	− 4.0 ± 1.0	− 17.5 ± 2.0	1.85 ± 0.44

* Errors in this column for + 40 mV are S.E.M. estimated from the scatter of I'_{rel} values. The *t* test was not performed on these populations.
† Indicates significant differences between data at + 40 and − 40 mV.
‡ Indicates significant differences between $I'_{F(peptideC)}$ and $I'_{F(control)}$.

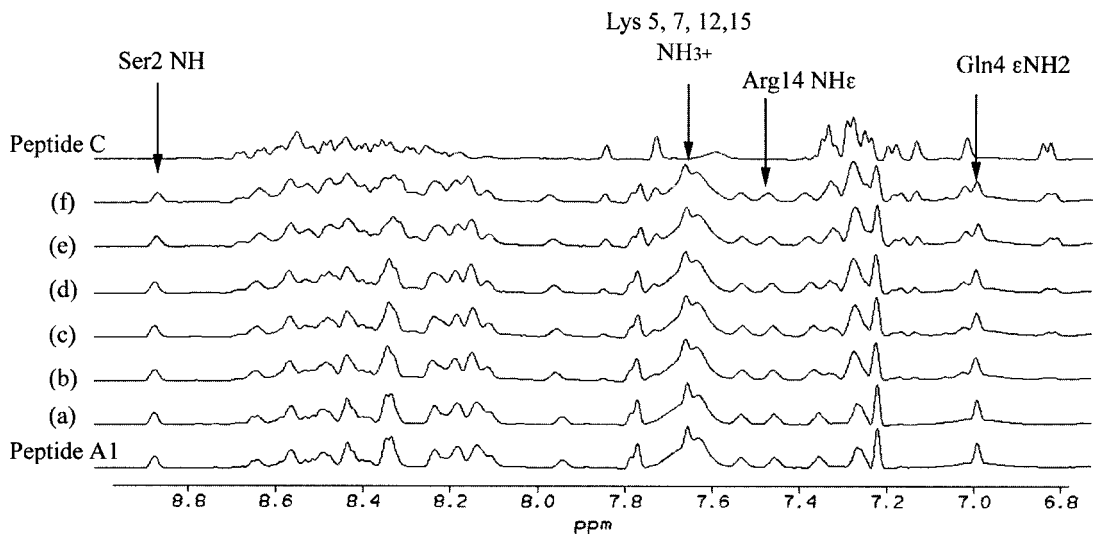

Figure 10 Peptides *C* and *A* do not associate in solution

A region of the ^{1}H-NMR spectra showing peaks associated with backbone and side-chain residues is shown. The uppermost spectrum shows data for peptide *C* alone, and the bottom spectrum shows peptide *A* alone, followed by addition of peptide *C* to *A* for final ratios of (spectrum a) 1 : 0.1, (spectrum b) 1 : 0.2, (spectrum c) 1 : 0.4, (spectrum d) 1 : 0.6, (spectrum e) 1 : 0.8 and (spectrum f) 1 : 1. Arrows denote the progress of peaks corresponding to a selection of isolated protons from peptide *A* (which have been previously assigned [15]) upon the addition of peptide *C*. Two of the labelled peaks include those belonging to positively charged residues in peptide *A* which could potentially interact with the negatively charged residues of peptide *C*. The peaks belonging to these positively charged side-chain residues should shift and broaden if an interaction between peptides *A* and *C* took place. No such shifts or broadening were detected.

produce peptide *A* activation of RyRs at low concentrations and voltage-dependent blockage at higher concentrations at + 40 mV (Figure 9 and Table 3). (iii) Peptide *A*, added to peptide *C*-activated channels, does not cause further average activation at − 40 mV (Figures 8B and 9B), and blocks channels at + 40 mV (Figure 9A and Table 3). (iv) Peptide *A*, added to channels inhibited by peptide *C*, does not activate the channels at − 40 mV to control levels or greater (where RyRs are normally activated by peptide *A*; see the subsection 'Inhibition by peptide *C* prevents activation of RyRs by ATP and peptide *A*' above). (v) Peptide *C*, added to channels that were activated by peptide *A* at − 40 mV, does not reduce the activation caused by peptide *A* (Figure 8A).

DISCUSSION

We describe two novel observations on the regulation of native skeletal RyRs by a peptide corresponding to the Glu^{724}–Pro^{760} region of the II–III loop of the skeletal muscle DHPR (peptide *C*). First, the peptide has two independent stochastic actions on single native skeletal RyR channels in lipid bilayers, namely inhibition and activation. These effects are slowly reversible, indicating a tight association between peptide *C* and the RyR complex. Secondly, the peptide has a random-coil structure in solution. Therefore the functional effects of the peptide can be interpreted in at least two ways. Peptide *C* may bind to independent activation and inhibition sites on the RyR complex. Alternatively, it may bind to a single site with activation requiring one peptide conformation and inhibition requiring a different conformation, as proposed for the effects of calmodulin on RyR activity [28]. The findings further suggest that both the activation and inhibition sites on the RyR targeted by peptide *C* are different from the activation and inhibition sites targeted by a second region of the II–III loop corresponding to peptide *A* (^{671}Thr–Lys^{690}).

The effects of peptide *C* reported here are associated with moderate binding affinities (0.1–150 μM) and with binding kinetics that are slower than seen with Ca^{2+} release during EC coupling. However, it is important to note that, in muscle, the II–III loop is likely to undergo a directed conformational change upon depolarization and repolarization of the T-tubule membrane so that the binding sites on the RyR would be effectively saturated by the II–III loop. In addition, the structure of the *C* region could be more stable in the intact DHPR and be more favourable for binding to the RyR. Thus accessibility may be more favourable *in vivo*, with the II–III loop anchored in an optimal position. The rates of loop binding would not then be limited by diffusion as they are in bilayer experiments, but only by the activation energy of the binding process. A naïve calculation of the rates of binding and unbinding of the *C* region of the II–III loop to RyRs in muscle can be made from the effective concentration of peptide *C* in the junctional gap ($\approx$5 mM [29]; although it is not clear that the II–III loop concentration has any meaning for the EC-coupling process for the reasons given above) and the kinetic rate constants obtained from the bilayer studies. At this concentration, the time constants for activation and inhibition of RyR by peptide *C* in lipid bilayers would be 20 μs and 30 ms respectively. Therefore the rates of activation and inhibition by peptide *C* are consistent with events that could occur during EC coupling. The slow reversal of inhibition by peptide *C* after perfusion suggests that, once bound, the peptide is strongly associated with the RyR and the dissociation rate is low. Since activation by peptide *C* shows the higher association rate, we speculate that activation is the most physiologically relevant effect. However, given that the peptide-binding kinetics could be much faster *in vivo*, the importance of an inhibitory action of the peptide cannot be discounted.

What do the effects of peptides on RyR activity mean in terms of DHPR–RyR interactions *in vivo*?

Activation of the RyR by the full II–III loop, or by loop peptides (both *A* and/or *C*), reflect protein–protein interactions between the DHPR fragments and the RyR. These effects show that regions of the II–III loop can bind to the RyR, but do not necessarily reflect regulation of the RyR by the DHPR during EC coupling. Indeed, it might be naïve to expect that the diffusion of a peptide to a bilayer and subsequent static binding of the peptide to the RyR could reflect the effects of dynamic conformational changes in the II–III loop on RyR activity during EC coupling. It is not known whether the interaction between the II–III loop and RyR occurs dynamically during EC coupling or whether there is a steady-state interaction between the proteins with conformational changes in the binding regions occurring during EC coupling. The idea of a steady-state interaction is appealing, since it would guarantee that the proteins are in the correct position for signalling to proceed. A steady-state interaction is consistent with observations that both the II–III loop and the loop peptides readily bind to, and do not easily unbind from, the RyR. The effects of binding of the loop fragments could reflect either the effects of the DHPR interactions with RyRs at rest or effects that occur during EC coupling, depending on whether the fragment conformation more closely resembles the resting or active conformation of the II–III loop *in situ*.

Mechanistic insights into the regulation of the RyR by the II–III loop provided by peptide studies

Previous peptide studies have shown that peptides *A* and *C* can activate the RyR *in vitro* and raise the possibility that the *C* region of the II–III loop may bind to the RyR complex and activate the channel *in vivo* [9–13,16]. The present results provide several additional mechanistic insights into regulation of the RyR by the DHPR II–III loop. These are listed here and discussed separately in later sections.

(i) First, we show that two regions (*A* and *C*) of the DHPR II–III loop can bind to the RyR complex by accessing at least two different sites. (ii) Secondly, we present the first evidence that the *C* region of the II–III loop can bind to the RyR complex and inhibit the channel, and that activation and inhibition by the *C* region are independent processes. (iii) Thirdly, we show that there are functional interactions between the *A* and *C* region binding sites so that (a) the *A* region cannot further activate RyRs that are activated by the *C* region and (b) that the *C* region does not cause further activation of RyRs activated by the *A* region. Thus additional activation is not achieved if both the *A* and *C* regions are bound. (d) Finally we show that peptide *A* cannot activate channels to control levels or above once are inhibited by peptide *C* (see the Results section), implying that there are functional interactions between the inhibitory site for peptide *C* and the activation site for peptide *A*. This ability of peptide *C* to over-ride the effects of peptide *A* may explain why the *A* region does not contribute to EC coupling in myocyte studies [6,8].

Independent activation and inhibition mechanisms for peptide *C*

The most compelling evidence that activation and inhibition by peptide *C* are independent processes is that in many instances either activation or inhibition was absent, i.e. a significant number of channels showed inhibition without preceding activation, while other channels activated by higher concentrations of peptide *C* did not show inhibition. The independence of activation or inhibition could have been due to the peptide either (a) binding to separate activation and inhibition sites or (b) binding to one site, sometimes in an activating conformation and at other times in an inhibiting conformation.

Separate activation and inhibition sites for peptides *A* and *C*

Several observations suggest that peptides *C* and *A* act at different sites on the RyR. The net negative charge on peptide *C* compared with a positive charge on peptide *A* suggests that the peptides might have difficulty in binding to the same activation or inhibition sites. Partial summation of activation by the peptides (both at maximally activating concentrations), in some individual channels (Figure 7A), suggests separate activation sites. Inhibition by peptide *A* is voltage-dependent and is likely to be due to interactions between the positive residues on the peptide and negative residues that line the pore [10,30]. Peptide *C* probably does not block the pore, since its inhibition is not voltage-dependent (Table 2) and its negative charges would be repelled by negative charges lining the pore. The activation/inhibition sites for peptide *C* and the activation site for peptide *A* are likely to be located on the cytoplasmic domain of the RyR complex, whereas the blocking site for peptide *A* is located in the RyR channel pore.

Inhibition by peptide *C*

Previous results [17] showed that peptide *C* prevented the activation of RyRs by peptide *A*. This could have been explained either by (i) the negatively charged peptide *C* binding to the positively charged peptide *A* and removing free peptide *A* from solution or (ii) by peptide *C* binding to the RyR and altering its response to peptide *A*. It is now clear that peptides *A* and *C* do not associate with each other in solution

and that peptide *C* can inhibit the RyR as well as depress the response to peptide *A*. Curiously, other studies show that a peptide containing the skeletal DHPR residues 720–765 does not inhibit purified RyR channels at concentrations $\leqslant 30\ \mu$M [13]. It is possible either that the additional five amino acids on the 720–765 peptide prevent its inhibitory effect or that the effect of the *C* region peptides differs between native and purified RyRs. The latter possibility could explain why purified RyRs do not bind peptide *C* in surface plasmon resonance studies [31], while native RyRs are crosslinked to peptide *C* in methylcoumarin acetate fluorescence studies [16]. Therefore associated proteins in the native RyR complex may alter the response to peptide *C*. Proteins such as triadin, calsequestrin and calmodulin can influence RyR activity [19,32–34], and might alter the response of RyRs to peptide *C*, either by influencing the binding of peptide *C* to the RyR or by binding to peptide *C* themselves.

Interactions between effects of peptide *A* and peptide *C*

The lack of average activation of RyRs by peptide *A* in the presence of peptide *C* can be attributed to summation of delayed inhibition by peptide *C* with activation by peptide *A* (Figure 8C). The observation that RyRs that were exposed to peptide *C* were on average not activated by peptide *A* (Figures 8B and 8C, and the text) is also consistent with peptide *C* preventing Ca^{2+} release from SR vesicles induced by peptide *A* [17]. On the other hand, the slow effects of peptide *C* on RyR channels are not consistent with its effects on SR vesicles [17]. In stopped-flow experiments, peptides *A* and *C* are added simultaneously and the immediate suppression of peptide *A*-induced activation of Ca^{2+} release suggests that peptide *C* bound to RyRs either before or simultaneously with peptide *A*. It is however possible that the association rates of the peptides with the RyR are vastly different under stopped-flow and bilayer conditions. The failure of peptide *C* alone to directly inhibit Ca^{2+} release from SR vesicles [14] can be explained by simultaneous activation of RyRs in some channels and inhibition in others, giving an overall null effect in the average data.

The physiological role of the *C* region of the II–III loop

Although it is tempting to interpret the effects on EC coupling of inserting skeletal sequences of the *A* and *C* regions into a cardiac II–III loop or scrambling the regions, in terms of parts of the DHPR that are involved in interactions between the DHPR and RyR as a part of dynamic steps in EC coupling [6,8,35], there are other explanations for the results of these experiments. For example, the fact that the 720–760 region of the II–III loop is essential for skeletal EC coupling may be because it is essential for the geometrical alignment of the DHPR and RyR [36]. Once aligned, structural and functional interactions between the DHPR and RyR may depend on other regions in the II–III loop and other domains of the DHPR and may not be skeletal-/cardiac-isoform-specific. This explanation is consistent with observations that recombinant II–III loops with either the cardiac or skeletal sequences can activate the RyR [9].

A complication with the models above is the recent observation that, although deletion of the *C* region of the II–III loop abolishes skeletal EC coupling and deletion of the *A* region alone has no effect, deletion of both *A* and *C* regions partially restores skeletal EC coupling [37]. An interpretation of these findings is that deletion of the *C* region induces a conformational change in the II–III loop that abolishes either EC coupling (or DHPR targeting) and that the structure was restored by also deleting the *A* region. The deletion studies can be reconciled with the chimaera studies [6,8,35] if it is assumed that the skeletal sequence in the *C* region is essential for a conformation of the II–III loop, which allows skeletal EC coupling (or targeting) to proceed. Since EC coupling was only partially restored by the $A + C$ deletion, it is possible that normal skeletal EC coupling (or proper targeting) requires the *C* region to both maintain II–III loop structure and to bind to the RyR. In any case, this finding strongly supports the hypothesis that multiple regions of the DHPR and RyR are involved in EC coupling.

Most models now suggest that there are multiple interaction sites on both the RyR and DHPR. This is not surprising given the massive size of the DHPR–RyR complex. Indeed, at least five macro regions of the DHPR are possibly important for its interaction with the RyR: the I–II loop [5], the III–IV loop [38], the C-terminal region of the DHPR [39], the β_1 subunit of the DHPR [40,41] and the II–III loop. Similarly, more than one region of the RyR interacts with the DHPR. Residues 1635–2635 are essential for skeletal-type EC coupling, whereas both 1635–2635 and 2659–3720 are required for retrograde signalling [42]. A fragment of the RyR including 1076–1112 contains a binding site for the II–III loop [43]. Further, more than one micro region within these large domains could be involved in interactions between the proteins, as seen with the *A* and *C* regions of the II–III loop.

In conclusion, we have demonstrated that a peptide corresponding to the *C* region of the DHPR II–III loop is a high-affinity activator and an inhibitor of the native skeletal muscle RyR. We also present evidence suggesting that at least two regions of the II–III loop of the DHPR can bind to separate sites on the RyR and that there are functional interactions between these binding sites when the loop regions are bound.

We are grateful to Suzy Pace and Joan Stivala for preparation and characterization of SR vesicles and to Dr Peter Jeffrey for assistance with equilibrium sedimentation experiments. D.L. was supported by the National Health & Medical Research Council of Australia (grant number 9936486).

REFERENCES

1 Fabiato, A. (1983) Calcium-induced release of calcium from the cardiac sarcoplasmic reticulum. Am. J. Physiol. **245**, C1–C14
2 Beuckelmann, D. J. and Wier, W. G. (1988) Mechanism of release of calcium from sarcoplasmic reticulum of guinea-pig cardiac cells. J. Physiol. (Cambridge, U.K.) **405**, 233–255
3 Nabauer, M., Callewaert, G., Cleemann, L. and Morad, M. (1989) Regulation of calcium release is gated by calcium current, not gating charge, in cardiac myocytes. Science **244**, 800–803
4 Armstrong, C. M., Bezanilla, F. M. and Horowicz, P. (1972) Twitches in the presence of ethylene glycol bis(-aminoethyl ether)-N,N′-tetracetic acid. Biochim. Biophys. Acta **267**, 605–608
5 Tanabe, T., Beam, K. G., Adams, B. A., Niidome, T. and Numa, S. (1990) Regions of the skeletal muscle dihydropyridine receptor critical for excitation-contraction coupling. Nature (London) **346**, 567–569
6 Nakai, J., Tanabe, T., Konno, T., Adams, B. and Beam, K. G. (1998) Localization in the II-III loop of the dihydropyridine receptor of a sequence critical for excitation-contraction coupling. J. Biol. Chem. **273**, 24983–24986
7 Ahern, C. A., Arikkath, J., Vallejo, P., Gurnett, C. A., Powers, P. A., Campbell, K. P. and Coronado, R. (2001) Intramembrane charge movements and excitation-contraction coupling expressed by two-domain fragments of the Ca^{2+} channel. Proc. Natl. Acad. Sci. U.S.A. **98**, 6935–6940
8 Wilkens, C. M., Kasielke, N., Flucher, B. E., Beam, K. G. and Grabner, M. (2001) Excitation-contraction coupling is unaffected by drastic alteration of the sequence surrounding residues L720-L764 of the alpha 1S II-III loop. Proc. Natl. Acad. Sci. U.S.A. **98**, 5892–5897
9 Lu, X., Xu, L. and Meissner, G. (1994) Activation of the skeletal muscle calcium release channel by a cytoplasmic loop of the dihydropyridine receptor. J. Biol. Chem. **269**, 6511–6516

10 Dulhunty, A. F., Laver, D. R., Gallant, E. M., Casarotto, M. G., Pace, S. M. and Curtis, S. (1999) Activation and inhibition of skeletal RyR channels by a part of the skeletal DHPR II-III loop: effects of DHPR Ser687 and FKBP12. Biophys. J. **77**, 189–203
11 Gurrola, G. B., Arevalo, C., Sreekumar, R., Lokuta, A. J., Walker, J. W. and Valdivia, H. H. (1999) Activation of ryanodine receptors by imperatoxin A and a peptide segment of the II-III loop of the dihydropyridine receptor. J. Biol. Chem. **274**, 7879–7886
12 Gallant, E. M., Curtis, S., Pace, S. M. and Dulhunty, A. F. (2001) Arg(615)Cys substitution in pig skeletal ryanodine receptors increases activation of single channels by a segment of the skeletal DHPR II-III loop. Biophys. J. **80**, 1769–1782
13 Stange, M., Tripathy, A. and Meissner, G. (2001) Two domains in dihydropyridine receptor activate the skeletal muscle Ca^{2+} release channel. Biophys. J. **81**, 1419–1429
14 el-Hayek, R., Antoniu, B., Wang, J., Hamilton, S. L. and Ikemoto, N. (1995) Identification of calcium release-triggering and blocking regions of the II-III loop of the skeletal muscle dihydropyridine receptor. J. Biol. Chem. **270**, 22116–22118
15 Casarotto, M. G., Gibson, F., Pace, S. M., Curtis, S. M., Mulcair, M. and Dulhunty, A. F. (2000) A structural requirement for activation of skeletal ryanodine receptors by peptides of the dihydropyridine receptor II-III loop. J. Biol. Chem. **275**, 11631–11637
16 Yamamoto, T., Rodriguez, J. and Ikemoto, N. (2002) Ca^{2+}-dependent dual functions of peptide C. The peptide corresponding to the Glu724-Pro760 region (the so-called determinant of excitation-contraction coupling) of the dihydropyridine receptor alpha 1 subunit II-III loop. J. Biol. Chem. **277**, 993–1001
17 Saiki, Y., el-Hayek, R. and Ikemoto, N. (1999) Involvement of the Glu724-Pro760 region of the dihydropyridine receptor II-III loop in skeletal muscle-type excitation- contraction coupling. J. Biol. Chem. **274**, 7825–7832
18 Ahern, G. P., Junankar, P. R. and Dulhunty, A. F. (1997) Subconductance states in single-channel activity of skeletal muscle ryanodine receptors after removal of FKBP12. Biophys. J. **72**, 146–162
19 Beard, N. A., Sakowska, M. M., Dulhunty, A. F. and Laver, D. R. (2002) Calsequestrin is an inhibitor of skeletal muscle ryanodine receptor calcium release channel. Biophys. J. **82**, 310–320
20 Dulhunty, A. F., Laver, D., Curtis, S. M., Pace, S., Haarmann, C. and Gallant, E. M. (2001) Characteristics of irreversible ATP activation suggest that native skeletal ryanodine receptors can be phosphorylated via an endogenous CaMKII. Biophys. J. **81**, 3240–3252
21 Haarmann, C. S., Laver, D. R. and Dulhunty, A. F. (2000) Effect of two different portions of the of the II-III loop of dihydropyridine receptor on single ryanodine receptors. In Proceeding of the National Physiological and Pharmacological Society, vol. 31 (McCance, I., ed.), p. 35P, Australian Physiological and Pharmacological Society, Melbourne, Vic
22 Ahern, G. P., Junankar, P. R. and Dulhunty, A. F. (1994) Single channel activity of the ryanodine receptor calcium release channel is modulated by FK-506. FEBS Lett. **352**, 369–374
23 Laver, D. R., Roden, L. D., Ahern, G. P., Eager, K. R., Junankar, P. R. and Dulhunty, A. F. (1995) Cytoplasmic Ca^{2+} inhibits the ryanodine receptor from cardiac muscle. J. Membr. Biol. **147**, 7–22
24 Sitsapesan, R. (1999) Similarities in the effects of DIDS, DBDS and suramin on cardiac ryanodine receptor function. J. Membr. Biol. **168**, 159–168
25 Laver, D. R., Eager, K. R., Taoube, L. and Lamb, G. D. (2000) Effects of cytoplasmic and luminal pH on Ca^{2+} release channels from rabbit skeletal muscle. Biophys. J. **78**, 1835–1851
26 O'Neill, E. R., Sakowska, M. M. and Laver, D. R. (2003) Regulation of the calcium release channel from skeletal muscle by Suramin and the disulfonated stilbene derivatives DIDS, DBDS, and DNDS. Biophys. J. **84**, 1–16
27 King, B. M. and Bear, G. (1993) Some (almost) assumption-free tests. In Statistical Reasoning in Psychology and Education (Minium, E. W., ed.), pp. 474–496, Wiley, New York
28 Rodney, G. G., Moore, C. P., Williams, B. Y., Zhang, J. Z., Krol, J., Pedersen, S. E. and Hamilton, S. L. (2001) Calcium binding to calmodulin leads to an N-terminal shift in its binding site on the ryanodine receptor. J. Biol. Chem. **276**, 2069–2074
29 Dulhunty, A. F., Haarmann, C. S., Green, D., Laver, D. R., Board, P. G. and Casarotto, M. G. (2002) Interactions between dihydropyridine receptors and ryanodine receptors in striated muscle. Progr. Biophys. Mol. Biol. **79**, 45–75
30 Mead, F. C., Sullivan, D. and Williams, A. J. (1998) Evidence for negative charge in the conduction pathway of the cardiac ryanodine receptor channel provided by the interaction of K^+ channel N-type inactivation peptides. J. Membr. Biol. **163**, 225–234
31 O'Reilly, F. M., Robert, M., Jona, I., Szegedi, C., Albrieux, M., Geib, S., De Waard, M., Villaz, M. and Ronjat, M. (2002) FKBP12 modulation of the binding of the skeletal ryanodine receptor onto the II-III loop of the dihydropyridine receptor. Biophys. J. **82**, 145–155
32 Kawasaki, T. and Kasai, M. (1994) Regulation of calcium channel in sarcoplasmic reticulum by calsequestrin. Biochem. Biophys. Res. Commun. **199**, 1120–1127
33 Tripathy, A., Xu, L., Mann, G. and Meissner, G. (1995) Calmodulin activation and inhibition of skeletal muscle Ca^{2+} release channel (ryanodine receptor). Biophys. J. **69**, 106–119
34 Ohkura, M., Furukawa, K., Fujimori, H., Kuruma, A., Kawano, S., Hiraoka, M., Kuniyasu, A., Nakayama, H. and Ohizumi, Y. (1998) Dual regulation of the skeletal muscle ryanodine receptor by triadin and calsequestrin. Biochemistry **37**, 12987–12993
35 Proenza, C., Wilkens, C. M. and Beam, K. G. (2000) Excitation-contraction coupling is not affected by scrambled sequence in residues 681–690 of the dihydropyridine receptor II-III loop. J. Biol. Chem. **275**, 29935–29937
36 Flucher, B. E. (2001) Molecular structure and assembly of the calcium release units in skeletal muscle. Proc. Int. Union Physiol. Sci. **XXXIV**, abstract 2942
37 Ahern, C. A., Bhattacharya, D., Mortenson, L. and Coronado, R. (2001) A component of excitation-contraction coupling triggered in the absence of the T671-L690 and L720-Q765 regions of the II-III loop of the dihydropyridine receptor alpha(1s) pore subunit. Biophys. J. **81**, 3294–3307
38 Jurkat-Rott, K., McCarthy, T. and Lehmann-Horn, F. (2000) Genetics and pathogenesis of malignant hyperthermia. Muscle Nerve **23**, 4–17
39 Slavik, K. J., Wang, J. P., Aghdasi, B., Zhang, J. Z., Mandel, F., Malouf, N. and Hamilton, S. L. (1997) A carboxy-terminal peptide of the alpha 1-subunit of the dihydropyridine receptor inhibits Ca(2+)-release channels. Am. J. Physiol. **272**, C1475–C1481
40 Beurg, M., Ahern, C. A., Vallejo, P., Conklin, M. W., Powers, P. A., Gregg, R. G. and Coronado, R. (1999) Involvement of the carboxy-terminus region of the dihydropyridine receptor beta1a subunit in excitation-contraction coupling of skeletal muscle. Biophys. J. **77**, 2953–2967
41 Beurg, M., Sukhareva, M., Ahern, C. A., Conklin, M. W., Perez-Reyes, E., Powers, P. A., Gregg, R. G. and Coronado, R. (1999) Differential regulation of skeletal muscle L-type Ca^{2+} current and excitation-contraction coupling by the dihydropyridine receptor beta subunit. Biophys. J. **76**, 1744–1756
42 Nakai, J., Sekiguchi, N., Rando, T. A., Allen, P. D. and Beam, K. G. (1998) Two regions of the ryanodine receptor involved in coupling with L-type Ca^{2+} channels. J. Biol. Chem. **273**, 13403–13406
43 Leong, P. and MacLennan, D. H. (1998) A 37-amino acid sequence in the skeletal muscle ryanodine receptor interacts with the cytoplasmic loop between domains II and III in the skeletal muscle dihydropyridine receptor. J. Biol. Chem. **273**, 7791–7794

Received 12 November 2002/13 February 2003; accepted 6 March 2003
Published as BJ Immediate Publication 6 March 2003, DOI 10.1042/BJ20021763